Available online at www.sciencedirect.com
ScienceDirect
Ceramics International 34 (2008) 505–510
CERAMICS INTERNATIONAL
www.elsevier.com/locate/ceramint

The effect of Al_2O_3 on sintering and crystallization of $MgSiO_3$-based glass-powder compacts

A. Goel [a], D.U. Tulyaganov [a,b], S. Agathopoulos [a], J.M.F. Ferreira [a,*]

[a] Department of Ceramics and Glass Engineering, University of Aveiro, CICECO, 3810-193 Aveiro, Portugal
[b] Scientific Research Institute of Space Engineering, 700128 Tashkent, Uzbekistan

Received 2 October 2006; received in revised form 28 October 2006; accepted 24 November 2006
Available online 21 December 2006

Abstract

The influence of Al_2O_3 (8 wt.%) on sintering and crystallization features of glass powders based on magnesium silicate ($MgSiO_3$) was experimentally determined. The investigated compositions were $Y_{0.125}Mg_{0.875}Si_{0.875}B_{0.125}O_3$ and $Y_{0.125}Mg_{0.725}Ba_{0.15}Si_{0.875}B_{0.125}O_3$. For the experiments, glasses in bulk and frit forms were produced by melting in Pt-crucible at 1600 °C for 1.5 h. Glass-powder compacts were sintered at different temperatures between 900 °C and 1100 °C. The evolution of crystalline regime was determined by in situ recording of X-ray diffractograms of fine glass powders at elevated temperatures. The results and their discussion showed that addition of 8 wt.% Al_2O_3 in glass batches affected the thermal properties of the glasses and resulted in $MgSiO_3$-based glass ceramics well sintered between 900 °C and 1100 °C. In the BaO-free $MgSiO_3$ glass ceramics, clino- and orthoenstatite crystallize while the presence of BaO favours the formation of hexacelsian.

Keywords: A. Sintering; D. Glass; D. Glass ceramics; Enstatite

1. Introduction

Magnesium metasilicate ($MgSiO_3$) has been extensively studied due to its abundance in the Earth's lower crust and upper mantle [1]. According to the review of Smith [2] and later by Lee and Heuer [3], $MgSiO_3$ occurs in three well characterised structures. Orthoenstatite (OE) and protoenstatite (PE) have orthorhombic symmetry and clinoenstatite (CE) monoclinic. The influence of the temperature and the time of annealing, the preparation route, the chemical nature and the amount of chemical dopants and the particle size of precursors on the phase transformations and the properties of $MgSiO_3$ have been comprehensively investigated [3–5].

The production of $MgSiO_3$ based materials via the glass-ceramic (GC) route features particular peculiarities because the precise stoichiometric composition of enstatite does not result in a stable glass. Lee and Heuler [3] have presented an attempt to produce stoichiometric $MgSiO_3$ glass by quenching of glass melt into water where liquid N_2 was bubbling. Heat treatment of powder from that glass with particles' diameter of about 180 μm at 800–1000 °C caused crystallization of OE, which was invariably associated with CE, independent on annealing time and cooling conditions (air, or water, or slow cooling of 5 K/min). At temperatures ≥1200 °C, PE formed at the expense of OE. During cooling, CE was formed. The sintered GC samples were highly porous, even after many hours of heat treatment at temperatures close to melting point.

Cooper et al. [6] melted and remelted stoichiometric $MgSiO_3$ composition at 1650 °C for 16 h to get high homogeneity. Nevertheless, during pouring into cold water the melt got an opalescence appearance, which, according to subsequent X-ray analysis, was due to traces of PE and OE. The produced cullet was pulverised to fine powder, sieved and annealed at temperatures between 1150 °C and 1200 °C for 24 h in air. The microstructure of annealed powder particles suggested columnar grain growth and surface crystallization mechanism (due to formation of centre voids).

The above mentioned studies [3,6] indicate that, to achieve control of glass crystallization, which will result in formation of enstatite, special glass compositions have to be designed [7]. In 1991, Beall [7,8] successfully developed GCs in the ternary $MgO–Al_2O_3–SiO_2$ system with tetragonal zirconia as nucleating

* Corresponding author. Tel.: +351 234 370242; fax: +351 234 425300.
E-mail address: jmf@cv.ua.pt (J.M.F. Ferreira).

0272-8842/$34.00
doi:10.1016/j.ceramint.2006.11.006

agent, where enstatite was the primary phase. Tetragonal zirconia was a distinguishable crystalline phase after heat treatment at 800 °C and 900 °C. Bulk nucleation and crystallization of PE occurred with heat treatment of the glasses at temperatures above 900 °C. During cooling, PE transformed into fine crystals of twinned CE.

Echeverria and Beall [7,9] have reported production of enstatite GCs via surface nucleation mechanism and sol–gel route. Their studies have also demonstrated that addition of BaO results in either celsian ($BaAl_2Si_2O_8$), or Ba-osumilite ($BaMg_2Al_6Si_9O_{30}$), depending on the Ba/Al ratio. In 1974, Takher et al. [10,11] developed steatite-based GCs in MgO–Al_2O_3–SiO_2 system by adding BaO and ZnO in glass batch, which exhibited wide sintering temperature range and improved dielectric properties. Partridge et al. and Budd [7,12–14] produced enstatite type GCs in the same ternary system using ZrO_2 and TiO_2 as nucleating agents. Surface nucleation and crystallization mechanisms governed the devitrification of glass powders.

Literature survey reveals that there is no systematic experimental documentation on the effect of Al_2O_3 on sintering and crystallization of $MgSiO_3$ based fine glass-powder compacts. In our earlier study [15], three glass compositions were melted in Al_2O_3 crucibles, aiming at producing Mg-metasilicate ($MgSiO_3$) based GCs. From that study, the first glass $Ca_{0.125}Mg_{0.875}SiO_3$, named as glass-1 and corresponding to a composition of 25 mol.% diopside ($CaMgSi_2O_6$) and 75 mol.% enstatite ($MgSiO_3$), was designed in such a way as to reduce the tendency of Mg-metasilicate for polymorphism [16]. With respect to $MgSiO_3$, in the second ($Y_{0.125}Mg_{0.875}Si_{0.875}B_{0.125}O_3$) and in the third ($Y_{0.125}Mg_{0.725}Ba_{0.15}Si_{0.875}B_{0.125}O_3$) [15]) glass compositions, substitutions of yttrium and barium for magnesium as well as boron for silicon were attempted. We met serious difficulties to produce stable glass of $Ca_{0.125}Mg_{0.875}SiO_3$ composition after 1 h dwelling at 1600 °C, which were, however, eliminated after prolongation of dwell time to 1.5–2 h, whereby homogenous and transparent glass-1 was obtained. Provided that sintering precedes crystallization in that system [15], heat treatment of glass-powder compacts at 850 °C for 1 h resulted in highly dense materials. Depending on the particular composition, CE and PE were developed at temperatures ≥850 °C and ≥900 °C, respectively.

Although the batches of the three above glasses did not contain Al_2O_3, in the BaO containing composition, hexacelsian ($BaAl_2Si_2O_8$) formed, which was attributed to a significant uptake of Al_2O_3 (6–7 wt.%) into the glass melt from the alumina crucibles. This finding suggested an active role of Al_2O_3 on the crystallization of GCs in the system of enstatite. The present study aims to shed light in the influence of Al_2O_3 on the sintering and crystallization features of glass powders with nominal compositions $Y_{0.125}Mg_{0.875}Si_{0.875}B_{0.125}O_3$ and $Y_{0.125}Mg_{0.725}Ba_{0.15}Si_{0.875}B_{0.125}O$ studied in our earlier study [15]. Therefore, the same glasses were melted in Pt crucibles. To distinguish the herein investigated glasses from those melted in Al_2O_3 crucibles and reported in our earlier study [15], their designations are 2a and 3a (which correspond to the glasses 2 and 3, respectively, of the earlier study [15]). Moreover, two more glasses, named as 2b and 3b, were also melted in Pt-crucibles, where 8 wt.% Al_2O_3 (i.e. close to the Al_2O_3-uptake in the earlier study [15]) was added in the compositions of the glasses 2a and 3a, respectively. For the sake of consistency with the previous study [15], small amount of NiO was also incorporated in the batches. Table 1 presents the compositions of the batches of the four investigated glasses.

Table 1
Compositions of batches of the investigated glasses (wt.%)

Glass	MgO	BaO	SiO_2	B_2O_3	Al_2O_3	Y_2O_3	NiO
2a	32.83	–	48.96	4.05	–	13.14	1.00
2b	30.21	–	45.05	3.73	8.00	12.09	0.92
3a	23.46	18.46	42.22	3.48	–	11.33	1.00
3b	21.59	16.99	38.85	3.21	8.00	10.44	0.92

2. Materials and experimental procedure

Powders of technical grade silicon oxide (purity >99.5%) and calcium carbonate (>99.5%), and of reactive grade Al_2O_3, H_3BO_3, MgO, Y_2O_3, $BaCO_3$, and NiO were used. Homogeneous mixtures of batches (∼100 g), obtained by ball milling, were preheated at 900 °C for 1 h for decarbonisation and then melted in Pt crucibles at 1600 °C for 1.5 h in air.

Glasses in bulk form of bars were produced by casting of the melts onto preheated bronze moulds and subsequent immediate annealing at 550 °C for 1 h. Glasses in frit form were also obtained by quenching of the melts in cold water. The frits were dried and then milled in a high-speed porcelain mill to obtain fine powders. The powders were granulated (by stirring in a mortar) in a 5 vol.% polyvinyl alcohol solution (PVA, Merck; the solution of PVA was made by dissolution in warm water) in a proportion of 97.5 wt.% of powder and 2.5 wt.% of PVA solution. Rectangular bars with dimensions of 4 mm × 5 mm × 50 mm were prepared by uniaxial pressing (80 MPa). The green bars were sintered at four different temperatures (i.e. 900 °C, 950 °C, 1000 °C and 1100 °C) in air. The soaking time at the sintering temperatures was 1 h, while a slow heating rate of 1 K/min aimed to prevent deformation of the samples.

In this study, the following techniques and apparatuses were employed. The particle size distribution of the fine powders from the frits was determined by light scattering technique (Coulter LS 230, UK, Fraunhofer optical model). These powders were subjected to differential thermal analysis in air (DTA, Labsys setaram TG-DTA/DSC; heating rate 5 K/min). Dilatometry measurements were done with as-cast-annealed bulk glass blocks (Bahr Thermo Analyse DIL 801 L, Germany; heating rate 5 K/min; cross-section of samples 4 mm × 5 mm).

The phase transformations occurring in fine glass powders over increasing temperature were monitored by in situ high temperature X-ray diffraction (HT-XRD) analysis (Philips, X'pert, The Netherlands, equipped with a Pt hot stage). The schedule of the hot stage was as follows: heating up to 600 °C with a rate of 10 K/min, heating with a rate of 5 K/min up to 900 °C, dwell for 30 min before recording the diffractogram, and then a similar ramp (5 K/min) and dwell (30 min) for

obtaining the diffractograms at 1000 °C and 1100 °C. Bars of glass-powder compacts sintered at different temperatures were also analyzed by X-ray diffraction (XRD) at room temperature (Rigaku Geigerflex D/Mac, C Series, Japan). In both cases of X-ray analysis, copper Kα radiation (λ = 1.5406 nm), produced at 30 kV and 25 mA, scanned the range of diffraction angles (2θ) between 10° and 80° with a 2θ-step of 0.02° s^{-1}. The phases were identified by comparing the experimental X-ray patterns to standards complied by the International Centre for Diffraction Data (ICDD).

Archimedes's method (i.e. immersion in diethyl-phthalate) was employed to measure the apparent density of the sintered samples (the mean values and the standard deviations presented have been obtained from 10 different samples). Rectified parallelepiped bars (3 mm × 4 mm × 50 mm) of sintered GCs were used for three-point bending strength measurements (Shimadzu Autograph AG 25 TA, 0.5 mm/min displacement; the mean values and their standard deviation presented have been obtained from measurements from 12 bars). The linear shrinkage due to sintering was calculated from the difference between the dimensions of the green bodies and the sintered samples (the mean values and the standard deviations presented have been obtained from 10 different samples).

3. Results

After 1.5 h of melting at 1600 °C, all the four investigated compositions were prone to easy casting and resulted in homogenous transparent glasses with dark honey colour (seemingly due to NiO) and no crystalline inclusions, as was also confirmed by X-ray analysis afterwards.

From the dilatometry curves of the cast-annealed bulk glasses, plotted in Fig. 1, the transition temperatures (T_g) and the dilatometric softening points (T_s) of the glasses were determined. The results, presented in Table 2, suggest that the presence of Al_2O_3 in the glasses (i.e. compositions 2b and 3b) causes a considerable reduction of T_g and T_s by about 80 °C and 40 °C, respectively, as compared to the Al_2O_3-free compositions (2a and 3a).

Alumina has also a strong impact in the DTA. Fig. 2 plots the results of DTA of fine powders with mean particle size of 2.8–3.0 μm, obtained from glass frits. With respect to the Al_2O_3-free glasses (2a and 3a), the presence of Al_2O_3 (2b and 3b) causes a shift to higher temperatures and an increase of intensity of the exothermic crystallization peak. Table 2 lists the temperatures of crystallization onset (T_c) and peak (T_p).

Table 2
Characteristic temperatures (in °C) and the difference $T_c - T_g$ for the investigated glasses, determined by analysis of dilatometry (Fig. 1) and DTA curves (Fig. 2)

Glass	T_g	T_s	T_c	T_p	$T_c - T_g$
2a	670	710	835	862	165
2b	590	670	870	898	280
3a	670	698	860	890	190
3b	610	653	895	928	285

The effect of Al_2O_3 was also sound in the properties of the sintered glass-powder compacts. In particular, the glass-powder compacts of the Al_2O_3-free compositions 2a and 3a were very poorly sintered after heat treatment at 900 °C and 1000 °C. The resultant samples of white colour were highly porous and extensively fractured. Therefore, any measurement of density and flexural strength would be worthless. Heat treatment at 1100 °C for 1 h slightly improved densification, but over-firing effect became evident because randomly distributed globules of grey-yellowish colour on the surface of the samples developed. In the contrast, the sintering ability of the Al_2O_3-containing samples 2b and 3b was very good. Completely dense samples with grey colour and smooth surfaces were obtained after heat treatment at 900 °C for 1 h. The appearance and the properties of the samples 2b and 3b were maintained after heat treatment at 950 °C for 1 h. The values of the properties, listed in Table 3, evidence the sound influence of Al_2O_3 on improving the properties of the produced GCs.

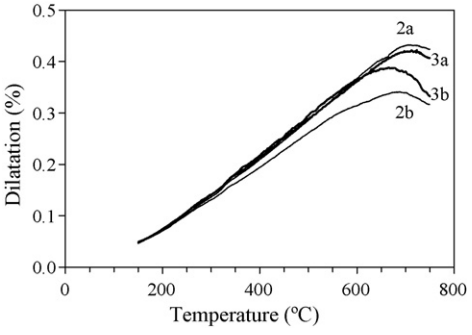

Fig. 1. Dilatometry curves obtained from as-cast and annealed bulk glasses.

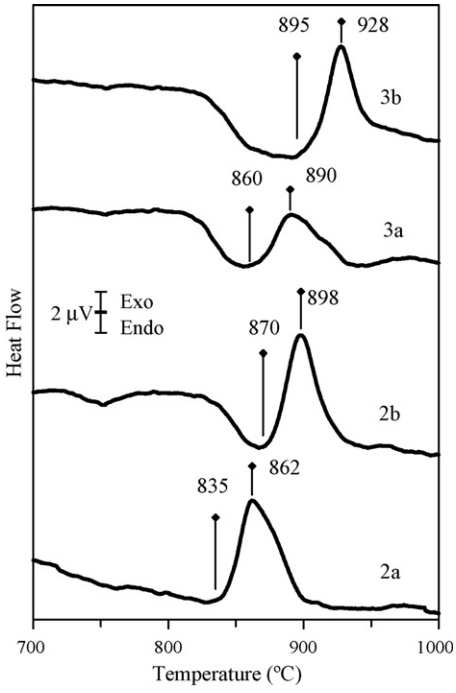

Fig. 2. Differential thermal analysis (DTA) of fine powders with mean particle size of 2.8–3.0 μm, obtained from glass frits of the investigated glasses.

Table 3
Properties of glass-ceramics (GC) produced after firing at different temperatures

GC	T (°C)	Shrinkage (%)	d (g/cm^3)	σ (MPa)
2a	1100	5.61 ± 0.18		19.64 ± 1.94
3a	1100	9.49 ± 0.34	2.31 ± 0.002	49.64 ± 1.52
2b	900	16.64 ± 0.47	3.07 ± 0.005	149.53 ± 34.79
3b	900	15.91 ± 0.30	3.20 ± 0.005	105.11 ± 24.41

Table 4
Evolution of crystalline phases assemblages in the investigated glasses over increasing temperature, determined by the high temperature X-ray diffraction (HT-XRD) analysis (Fig. 3)

Glass	900 °C	1000 °C	1100 °C
2a	CE, OE	CE, OE	CE, OE, PE, K
3a	OE, CE	OE, CE	
2b	PE, CE, Q	PE, CE, Q	PE; CE; Q
3b	CE, OE, HC	CE, PE, OE, HC	

CE: clinoenstatite; OE: orthoenstatite; PE: protoenstatite; K: kevyite; Q: quartz; HC: hexacelsian.

Fig. 3 presents in detail the evolution of the crystalline regime of the four investigated compositions by plotting a narrow range of 2θ angles (15–40°) of the X-ray diffractograms obtained in situ at the high temperatures (HT-XRD) from the fine glass powders, similar to those used for DTA. In the diagrams of Fig. 3, the patterns of the standard crystalline phases, compiled by ICDD and employed for the phases' identification, are also plotted. To be consistent with the work of Lee and Heuler [3], in this study we have used the ICDD cards 00-019-0768 for OE, 00-019-0769 for CE, and 00-011-273 for PE. For PE, we have also used the cards 01-086-0432 and 01-086-0434 (marked as PE* and PE**, respectively, in Fig. 3b). It should be also mentioned that since the diffractograms of synthetic CE and OE are quite similar, we have considered the peak corresponding to 0.298 nm (2θ = 30.001°) for securing the presence of CE [3].

Regarding the Al_2O_3-free compositions 2a and 3a, the HT-XRD analysis at 900 °C, 1000 °C, and 1100 °C shows that CE and OE precipitate from the glass 2a at 900 °C. The intensity of the peaks slightly increases at 1000 °C. Peaks of PE and keivyite ($Y_2Si_2O_7$, ICDD card 00-022-1103, marked as K in Fig. 3a) were registered in the diffractogram of 1100 °C. PE predominantly crystallizes from the glass 3a at all investigated temperatures, along with quartz (ICDD card 01-081-1665, marked as Q in Fig. 3b) and CE as secondary phases. The intensity of the peaks of PE and quartz are reduced at 1100 °C, likely due to dissolution effect in liquid phase. The HT-XRD peaks of sample 3a at 2θ values of 27.065 and 28.685 were considered belonging to an unknown phase.

Our earlier study [15] with analogous glasses has shown that heating at temperatures higher than 1000 °C causes significant increase of liquid phase fraction. Therefore, HT-XRD analysis of the Al_2O_3-contaning compositions 2b and 3b was carried out only at 900 °C and 1000 °C. According to the diffractograms shown in Fig. 3, OE and CE precipitate from the glass 2b at 900 °C, while there is no evidence of formation of other phases. The same phase assemblage develops after heat treatment at 1000 °C with no significant alterations of $MgSiO_3$-polymorphs' peaks intensity. In the case, however, of the glass 3b, hexacelsian (ICDD card 01-088-1051, marked as HC in Fig. 3b) was largely crystallised at 900 °C, while the intensity of the CE and OE peaks were quite low. There are no sound differences in the diffractogram of 3b at 1000 °C except the low intensity peaks of PE registered. Table 4 concisely summarizes

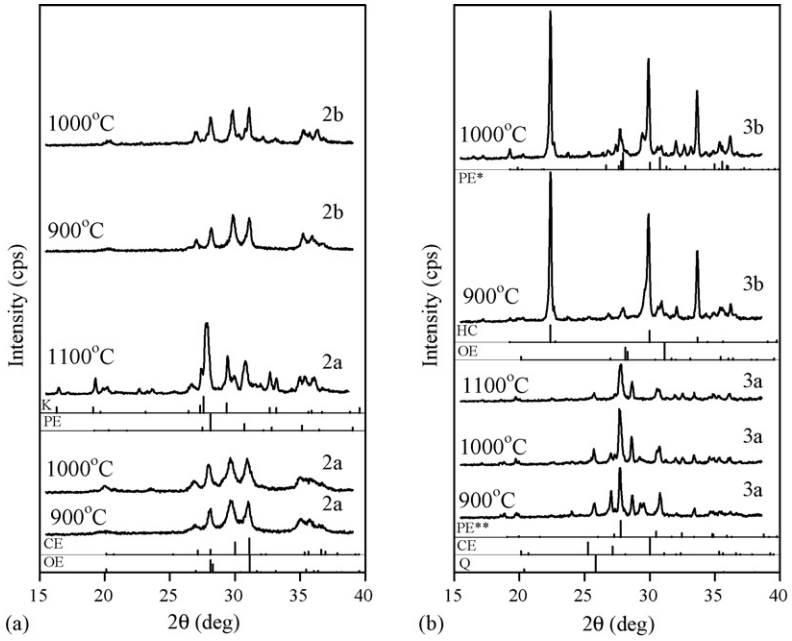

Fig. 3. X-ray diffractograms of fine glass-powders obtained in situ at high temperatures (HT-XRD). (For phases abbreviations and their ICDD cards see the text. The diffractograms have not been normalized. Full scale of intensity axis 8000 cps.)

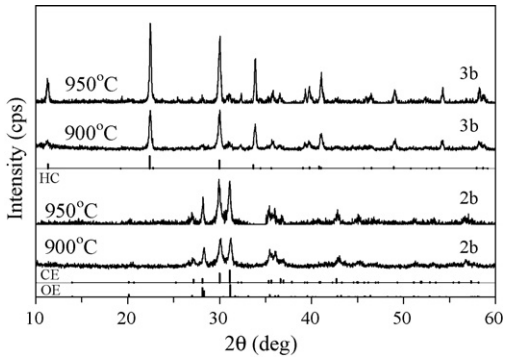

Fig. 4. X-ray diffractograms of glass-powder compacts of the Al_2O_3-contaning compositions 2b and 3b sintered at 900 °C and 950 °C. (For phases abbreviations and their ICDD cards see the text. The diffractograms have not been normalized. Full scale of intensity axis 1200 cps.)

the phase assemblages determined by the HT-XRD analysis (Fig. 3).

The X-ray diffractograms of the Al_2O_3-containing GCs (2b and 3b), sintered at 900 °C and 950 °C for 1 h and then cooled to room temperature, are plotted in Fig. 4. Sintered GCs 2b comprise CE and OE, while the peaks of hexacelsian dominate in the diffractograms of GCs 3b together with less intensive peaks of CE and OE.

4. Discussion

The experimental results of this study agree fairly well with earlier studies outlined in Section 1 and summarized in the difficulties of producing stable glass with composition of $MgSiO_3$ and the remarkable delay of densification of the Al_2O_3-free $MgSiO_3$. This was the main reason that many researches have shifted their interest in the $MgO–Al_2O_3–SiO_2$ system to produce sintered $MgSiO_3$ GCs. Indeed, high quality $MgSiO_3$ GCs have been produced from glass powders via surface nucleation and crystallization mechanisms with batches based on $MgO–Al_2O_3–SiO_2$ system and additions of ZrO_2, TiO_2, ZnO, and BaO [7,9–11,14].

The results of the present study demonstrated that addition of Al_2O_3 outstandingly improves densification of $MgSiO_3$-based glass-powder compacts (Table 3). It has been well documented [17–20] that densification of glass-powder compacts is initially achieved through viscous flow at temperatures slightly higher than T_g. Accordingly, the lowering of T_g in the case of the Al_2O_3-containing glasses 2b and 3b (Table 2) shifts sintering to lower temperatures comparing to the Al_2O_3-free glasses 2a and 3a.

In general, the desired order of events in glass-powder densification process occurs when sintering precedes crystallization. However, densification process does not always follow that sequence because crystallization stage may take place before or simultaneously with sintering stage [17]. Hence, glasses with large temperature interval between T_g and T_c (crystallization onset temperature) can possibly be well sintered [18]. In the present study, the effect of Al_2O_3 on improving densification of $MgSiO_3$ based glass-powder compacts can be explained since it favours the widening of temperature gap between T_g and T_c (Table 2).

With the aid of literature sources, the above discussed effects of Al_2O_3 might be due to the lower field strength of the large Al^{3+} ions, which could cause Al^{3+}-substitution for Si^{4+} in the tetrahedral positions of the glass network. This substitution can result at lowering of T_g and in a weakening effect in the cross-linking within the glass network [20]. The occurrence of natural OE together with ~7 wt.% Al_2O_3 [3] supports the above suggestion for such a substitution. The role of Al_2O_3 can be also implicated in the diffusion mechanism. It has been reported [21] that Al_2O_3 affects the diffusion mechanism at the initial stages of sintering, causing a decrease of activation energy of diffusion. However, further studies are necessary to understand this mechanism in detail for the investigated glass compositions.

With regards to the phases crystallized from the investigated glasses (Table 4, Figs. 3 and 4), the GCs 2a and 2b sintered at temperatures ≤1000 °C comprise OE and CE, while PE forms in GCs 2a at temperatures >1000 °C. It is worthy noting that no alumina-associated phase was registered in the diffractograms of 2b, suggesting stabilization of OE by Al_2O_3 [3] along with stabilization of CE. Moreover, no Y_2O_3 associated phases were recorded in the diffractograms (except in 2a at 1100 °C, Fig. 3a), suggesting possible Y-substitution for Mg, as has been also considered in our earlier study [15]. The presence of BaO seemingly favours the early formation (≥900 °C) of PE in the Al_2O_3-free GCs 3a and the formation of hexacelsian in the Al_2O_3-containing 3b GCs.

As it has already mentioned, this study was largely motivated for skipping the drawback of our earlier study [15] related to the significant (6–7 wt.%) uptake of Al_2O_3 into the glass melts from the alumina crucibles. Therefore, the compositions 2b and 3b were melted in Pt crucibles to reproduce the compositions 2 and 3 of our earlier study [15] at the certain extent. Comparison of the values of the properties (Table 3) as well as the crystalline phases formed (Table 4, Figs. 3 and 4) after heat treatment allows us to claim that this aim was practically achieved. However, in that earlier study [15], we have assumed the presence of only CE (the XRD patterns of synthetic CE and OE are close to one to the other, and thus we considered the peak of 0.298 nm as diagnostic for the presence of CE).

5. Conclusions

This study has experimentally determined the influence of Al_2O_3 on sintering and crystallization of glass-powder compacts which have nominal compositions of $Y_{0.125}Mg_{0.875}Si_{0.875}B_{0.125}O_3$ and $Y_{0.125}Mg_{0.725}Ba_{0.15}Si_{0.875}B_{0.125}O_3$. The addition of 8 wt.% Al_2O_3 in glass batches decreases T_g and T_s and increases the difference $T_c - T_g$, resulting, therefore, in well sintered $MgSiO_3$-based glass ceramics of high quality. The relevant Al_2O_3-free glass-powders compacts were poorly sintered between 900 °C and 1100 °C. Clino- and orthoenstatite are stable in the presence of Al_2O_3 in the BaO-free $MgSiO_3$ glass ceramics. The presence of BaO favours the early

formation ($\geq$900 °C) of proto-enstatite from the Al_2O_3-free $MgSiO_3$ glasses and hexacelsian formation in the Al_2O_3-containing glasses.

Acknowledgements

The financial support of CICECO (A. Goel) and FCT (S. Agathopoulos, project SFRH/BPD/1619/2000) are gratefully acknowledged.

References

[1] F. Nestola, G.D. Gatta, T.B. Ballaran, The effect of Ca substitution on the elastic and structural behaviour of orthoenstatite, Am. Mineral. 91 (2006) 809–815.
[2] J.V. Smith, Crystal structure and stability of the $MgSiO_3$ polymorphs: physical properties and phase relations of Mg, Fe pyroxens, Miner. Soc. Am. Spec. Pap. 2 (1969) 3–29.
[3] W.E. Lee, A.H. Heuer, On the polymorphism of enstatite, J. Am. Ceram. Soc. 70 (1987) 349–360.
[4] C.M. Huang, D.H. Kuo, Y.J. Kim, W. Kriven, Phase stability of chemically derived enstatite ($MgSiO_3$) powders, J. Am. Ceram. Soc. 77 (1994) 2625–2631.
[5] W. Mielcarek, D. Nowak-Wozny, K. Prociow, Correlation between $MgSiO_3$ phases and mechanical durability of steatite ceramics, J. Eur. Ceram. Soc. 24 (2004) 3817–3821.
[6] R.F. Cooper, W.Y. Yoon, J.H. Perepezko, Internal nucleation of high undercooled magnesium metasilicate melts, J. Am. Ceram. Soc. 74 (1991) 1312–1319.
[7] W. Höland, G.N. Beall, Glass-Ceramic Technology, The American Ceramic Society, Westerville, Ohio, 2002.
[8] G.N. Beall, Refractory glass-ceramic containing enstatite, US Patent 4,687,749 (18th August 1987).
[9] L.M. Echeverria, G.N. Beall, Enstatite ceramics; glass and gel routes, in: K.M. Nair (Ed.), Glasses for Electronic applications, Ceram. Trans., vol. 20, American Ceramic Society, Westerville, OH, 1991, pp. 235–244.
[10] E.A. Takher, T.I. Fedoseeva, V.Yu. Kellerman, R.Ya. Popilsky, High-strength steatite ceramics with broad range of the sintering stage, Glass Ceram. 2 (1974) 19–21.
[11] E.A. Takher, R. Ya Popilsky, V. Yu Kellerman, A.G. Sokolnikova, Dielectric steatite ceramics, Glass Ceram. 10 (1975) 19–21.
[12] G. Partridge, M.I. Budd, Toughened glass-ceramics, UK Patent GB 2172282 (17 September 1986).
[13] G. Partridge, M. Elyard, M.I. Budd, Glass-ceramics in substrate applications, in: M.H. Levis (Ed.), Glasses and Glass-Ceramics, Chapman and Hall, London, UK, 1989, pp. 226–271.
[14] M.I. Budd, Sintering and crystallization of a glass powder in the MgO–Al_2O_3–SiO_2–ZrO_2 system, J. Mater. Sci. 28 (1993) 1007–1014.
[15] A. Goel, D.U. Tulyaganov, S. Agathopoulos, M.J. Ribeiro, J.M.F. Ferreira, Synthesis and characterization of $MgSiO_3$-containing glass-ceramics, Ceram. Int. 33 (2007) 1481–1487.
[16] V.I. Vereshchagin, E.P. Tzymbalyuk, B.P. Romanov, Correlation between crystalline structure and physico-technical properties of solid solutions in the system clinoenstatite-diopside, in: Nucleated Crystallization of Glasses, State Institute of Glass, Moscow, 1982 pp. 95–100 (in Russian).
[17] C. Silgardi, M.C. D'Arrigo, C. Leonelli, Sintering behaviour of glass ceramics frits, Am. Ceram. Soc. Bull. 9 (2000) 88–93.
[18] Y.M. Sung, The effect of additives on the crystallization and sintering of $2MgO–2Al_2O_3–5SiO_2$ glass-ceramics, J. Mater. Sci. 31 (1996) 5421–5427.
[19] C. Lira, A.P.N. Oliveira, O.E. Alarcon, Sintering and crystallization of $CaO–Al_2O_3–SiO_2$ glass powder compacts, Glass Technol. 42 (2001) 91–96.
[20] A. Rosenflanz, M. Frey, B. Endres, T. Anderson, E. Richards, C. Schardt, Bulk glasses and ultrahard nanoceramics based on alumina and rare-earth oxides, Nature 430 (2004) 761–764.
[21] K. Matsuai, N. Ohmichi, M. Ohgai, Sintering kinetics at constant rates of heating: effect of Al_2O_3 on the initial sintering stage of fine zirconia powder, J. Am. Ceram. Soc. 88 (2005) 3346–3352.